Quantum Monte Carlo calculations of weak transitions in $A = 6$–10 nuclei

S. Pastore[a], A. Baroni[b], J. Carlson[a], S. Gandolfi[a], Steven C. Pieper[d], R. Schiavilla[b,c], and R.B. Wiringa[d]
[a] *Theoretical Division, Los Alamos National Laboratory, Los Alamos, NM 87545*
[b] *Department of Physics, Old Dominion University, Norfolk, VA 23529*
[c] *Theory Center, Jefferson Lab, Newport News, VA 23606*
[d] *Physics Division, Argonne National Laboratory, Argonne, IL 60439*
(Dated: August 24, 2017)

Ab initio calculations of the Gamow-Teller (GT) matrix elements in the β decays of ^{6}He and ^{10}C and electron captures in ^{7}Be are carried out using both variational and Green's function Monte Carlo wave functions obtained from the Argonne v_{18} two-nucleon and Illinois-7 three-nucleon interactions, and axial many-body currents derived from either meson-exchange phenomenology or chiral effective field theory. The agreement with experimental data is excellent for the electron captures in ^{7}Be, while theory overestimates the ^{6}He and ^{10}C data by $\sim 2\%$ and $\sim 10\%$, respectively. We show that for these systems correlations in the nuclear wave functions are crucial to explain the data, while many-body currents increase by $\sim$ 2–3% the one-body GT contributions. These findings suggest that the longstanding g_A-problem, *i.e.*, the systematic overprediction ($\sim 20\%$ in $A \leq 18$ nuclei) of GT matrix elements in shell-model calculations, may be resolved, at least partially, by correlation effects.

PACS numbers: 21.45.-v, 23.40-s

A major objective of nuclear theory is to explain the structure and dynamics of nuclei in a fully microscopic approach. In such an approach the nucleons—the nucleus' constituents—interact with each other in terms of many-body (primarily, two- and three-body) effective interactions, and with external electroweak probes via effective currents describing the coupling of these probes to individual nucleons and many-body clusters of them. We will refer below to this approach as the *basic model* of nuclear theory.

For light nuclei (s- and p-shell nuclei up to ^{12}C), quantum Monte Carlo (QMC) and, in particular, Green's Function Monte Carlo (GFMC) methods allow us to carry out first-principles, accurate calculations of a variety of nuclear properties [1–3] within the basic model. These calculations retain the full complexity of the many-body correlations induced by the Hamiltonians and currents, which have an intricate spin-isospin operator structure. When coupled to these numerically accurate QMC methods, the deceptively simple picture put forward in the basic model provides a quantitative and accurate description of the structure and dynamics of light nuclei over a broad energy range, from the keV's relevant in nuclear astrophysical contexts [3–5], to the MeV's of low-lying nuclear spectra [3, 6] and radiative decay processes [2, 7], to the GeV's probing the short-range structure of nuclei and the limits of the basic model itself [2, 8–10].

In the present study we focus on low-energy weak transitions in nuclei with mass number $A = 6$–10. To the best of our knowledge, calculations of β-decays and electron-capture processes in this mass range have relied so far, with the exception of Refs. [11, 12] discussed below and of Ref. [13] reporting on the ^{6}He β-decay, on relatively simple shell-model or cluster descriptions of the nuclear states involved in the transitions. The shell model—itself an approximation of the basic model—has typically failed to reproduce the measured Gamow-Teller (GT) matrix elements governing these weak transitions, unless use was made of an effective one-body GT operator, in which the nucleon axial coupling constant g_A is quenched relative to its free value [14, 15] (ranging from $g_A^{\rm eff} \simeq 0.85\, g_A$ in the light nuclei under consideration here to $g_A^{\rm eff} \simeq 0.7\, g_A$ in heavy nuclei). More phenomenologically successful (and less so) models have been based on α-nucleon-nucleon (for A=6) or α-^{3}H and α-^{3}He (for A=7) or α-α-nucleon-nucleon (for A=10) clusterization, and have used Faddeev techniques with a separable representation of the nucleon-nucleon and α-nucleon interaction [16] or the resonating-group method [17] or rather crude potential wells [18]. While these studies provide useful insights into the structure of these light systems, nevertheless their connection to the basic model is rather tenuous. In particular, they do not explain whether the required quenching of g_A in shell-model calculations reflects deficiencies in the corresponding wave functions—possibly due to the lack of correlations and/or to limitations in model space—or in the model adopted for the nuclear axial current, in which many-body terms are typically neglected.

The first QMC calculation of the $A = 6$–7 weak transitions in the basic model was carried out with the Variational Monte Carlo (VMC) method in Ref. [11]. It used nuclear axial currents including, apart from the (one-body) GT operator, two-body operators, which arise naturally in a meson-exchange picture (π- and ρ-exchange, and $\rho\pi$-transition mechanisms) and when excitations of nucleon resonances (notably the Δ isobar) are taken into account. These two-body operators, multiplied by hadronic form factors so as to regularize their short-range behavior in configuration space, were then constrained to reproduce the GT matrix element contributing to tritium β decay by adjusting the poorly known N-to-Δ axial coupling constant (see Ref. [19] for a recent summary).

Yet, the calculations of Ref. [11] were based on *approximate* VMC wave functions to describe the nuclear states involved in the transitions. This shortcoming was remedied in the subsequent GFMC study of Ref. [12], which, however, only retained the one-body GT operator. Adding to the GFMC-calculated one-body matrix elements the VMC estimates of two-body contributions obtained in Ref. [11] led Pervin *et al.* [12] to speculate that a full GFMC calculation of these $A=6$–7 weak transitions might be in agreement with the measured values.

The last three decades have witnessed the emergence of chiral effective field theory (χEFT) [20]. In χEFT, the symmetries of quantum chromodynamics (QCD), in particular its approximate chiral symmetry, are used to systematically constrain classes of Lagrangians describing, at low energies, the interactions of baryons (nucleons and Δ isobars) with pions as well as the interactions of these hadrons with electroweak fields [21, 22]. Thus χEFT provides a direct link between QCD and its symmetries, on one side, and the strong and electroweak interactions in nuclei, on the other. Germane to the subject of the present letter are, in particular, the recent χEFT derivations up to one loop of nuclear axial currents reported in Refs. [23, 24]. Both these studies were based on time-ordered perturbation theory and a power-counting scheme *à la* Weinberg, but adopted different prescriptions for isolating non-iterative terms in reducible contributions. There are differences—the origin of which is yet unresolved—in the loop corrections associated with box diagrams in these two independent derivations.

The present study reports on VMC and GFMC calculations of weak transitions in ^{6}He, ^{7}Be, and ^{10}C, based on the Argonne v_{18} (AV18) two-nucleon [25] and Illinois-7 (IL7) three-nucleon [26] interactions, and axial currents obtained either in the meson-exchange [19] or χEFT [23] frameworks mentioned earlier. The AV18+IL7 Hamiltonian reproduces well the observed spectra of light nuclei ($A=3$–12), including the ^{12}C ground- and Hoyle-state energies [3]. The meson-exchange model for the nuclear axial current has been most recently reviewed in Ref. [19], where explicit expressions for the various one-body (1b) and two-body (2b) operators are also listed (including fitted values of the N-to-Δ axial coupling constant). The χEFT axial current [23, 27] consists of 1b, 2b, and three-body (3b) operators. The 1b operators read

$$\mathbf{j}^{\rm 1b}_{5,\pm} = -g_A \sum_{i=1}^{A} \tau_{i,\pm} \left(\boldsymbol{\sigma}_i - \frac{\boldsymbol{\nabla}_i \; \boldsymbol{\sigma}_i \cdot \boldsymbol{\nabla}_i - \boldsymbol{\sigma}_i \, \nabla_i^2}{2\, m^2} \right) , \quad (1)$$

where $\tau_{i,\pm} = (\tau_{i,x} \pm i\, \tau_{i,y})/2$ is the standard isospin raising (+) or lowering (−) operator, and $\boldsymbol{\sigma}_i$ and $-i\, \boldsymbol{\nabla}_i$ are, respectively, the Pauli spin matrix and momentum operator of nucleon i. The 2b and 3b operators are illustrated diagrammatically in Fig. 1 in the limit of vanishing momentum transfer considered here. Referring to Fig. 1, the 2b operators are from contact [CT, panel (a)], one-pion exchange (OPE) [panels (b) and (f)], and multi-pion exchange (MPE) [panels (c)-(e) and (g)],

$$\mathbf{j}^{\rm 2b}_{5,\pm} = \sum_{i<j=1}^{A} \Big[\mathbf{j}^{\rm CT}_{5,\pm}(ij) + \mathbf{j}^{\rm OPE}_{5,\pm}(ij) + \mathbf{j}^{\rm MPE}_{5,\pm}(ij) \Big] \; , \quad (2)$$

and the 3b operators are from MPE [panels (h)-(i)],

$$\mathbf{j}^{\rm 3b}_{5,\pm} = \sum_{i<j<k=1}^{A} \mathbf{j}^{\rm MPE}_{5,\pm}(ijk) \; . \quad (3)$$

Configuration-space expressions for these 2b and 3b operators are reported in Ref. [27].

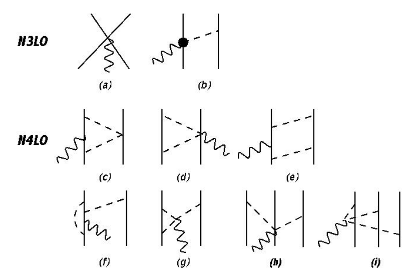

FIG. 1. Diagrams illustrating the (non-vanishing) contributions to the 2b and 3b axial currents. Nucleons, pions, and external fields are denoted by solid, dashed and wavy lines, respectively. The circle in panel (b) represents the vertex implied by the $\mathcal{L}^{(2)}_{\pi N}$ chiral Lagrangian [28], involving the LECs c_3 and c_4. Only a single time ordering is shown; in particular, all direct- and crossed-box diagrams are accounted for. The power counting of the various contributions is also indicated. See text for further explanations.

The 1b operator in Eq. (1) includes the leading order (LO) GT term and the first non-vanishing corrections to it, which come in at next-to-next-to-leading order (N2LO) [27]. Long-range 2b corrections from OPE enter at N3LO, panel (b) in Fig. 1, involving the low-energy constants (LECs) c_3 and c_4 in the sub-leading $\mathcal{L}^{(2)}_{\pi N}$ chiral Lagrangian [28], as well as at N4LO, panel (f). In terms of the expansion parameter Q/Λ_χ—where Q specifies generically the low-momentum scale and $\Lambda_\chi=1$ GeV is the chiral-symmetry-breaking scale—they scale as $(Q/\Lambda_\chi)^3$ and $(Q/\Lambda_\chi)^4$, respectively, relative to the LO. Loop corrections from MPE, panels (c)-(e) and (g), come in at N4LO, as do 3b currents, panels (h)-(i). Finally, the contact 2b current at N3LO, panel (a), is proportional to a LEC, denoted as z_0.

The short-range behavior of the 2b and 3b operators is regularized by including a cutoff $C_\Lambda(k) = \exp(-k^4/\Lambda^4)$ in momentum space [27], and the values $\Lambda = 500$ and 600 MeV are considered in the present work. In correspondence to each Λ and to each set of (c_3, c_4), either

$(c_3, c_4) = (-3.2, 5.4)$ GeV^{-1} as reported in Ref. [29] or $(c_3, c_4) = (-5.61, 4.26)$ GeV^{-1} as determined in Ref. [30], the LEC z_0 is constrained to reproduce the measured GT matrix element of tritium in hyperspherical-harmonics calculations based on the AV18+UIX Hamiltonian [27]. While the three-nucleon potential employed in that work, the Urbana IX (UIX) model [31], is different from the IL7 adopted here, nevertheless both Hamiltonians, AV18+UIX and AV18+IL7, reproduce the empirical values for the trinucleon binding energies and charge radii. In particular, we find that the AV18+IL7-calculated tritium GT matrix element with VMC is within $\lesssim 1.5\%$ of the experimental determination.

Reduced matrix elements (RMEs) for the β decays between the ^{6}He$(0^+;1)$ and ^{6}Li$(1^+;0)$ ground states, and between the ^{10}C$(0^+;1)$ ground state and ^{10}B$(1^+;0)$ first excited state, and ϵ captures of the ^{7}Be$(3/2^-;1/2)$ ground state to the ^{7}Li$(3/2^-;1/2)$ ground state and ^{7}Li$(1/2^-;1/2)$ first excited state are listed in Table I (in parentheses are the spin-parity, J^π, and isospin, T, assignments for each state). All processes are allowed or superallowed, and are therefore driven (almost) exclusively by the axial current (and, additionally, the vector charge—the Fermi operator—for the transition between the ground states of ^{7}Be and ^{7}Li). Retardation effects from the momentum transfer dependence of the operators, and corrections from suppressed transitions, such as, for example, those induced in the $A=6$ and 10 decays by the magnetic dipole associated with the vector current, are negligible [11]. Therefore the RMEs listed in Table I follow simply from

$$\mathrm{RME} = \frac{\sqrt{2\,J_f+1}}{g_A}\,\frac{\langle J_f M | j^z_{5,\pm} | J_i M\rangle}{\langle J_i M, 10 | J_f M\rangle}\;, \tag{4}$$

where $j^z_{5,\pm}$ is the z-component of the axial current $\mathbf{j}_{5,\pm}$ (at vanishing momentum transfer) given above and $\langle J_i M, 10 | J_f M\rangle$ are Clebsch-Gordan coefficients. The VMC results are obtained by straightforward Monte Carlo integration of the nuclear matrix elements above between (approximate) VMC wave functions; the GFMC results are from mixed-estimate evaluations of these matrix elements using previously generated GFMC configurations for the states under consideration, as illustrated in Ref. [12].

	^{6}He β-decay	^{7}Be ϵ-capture (gs)	^{7}Be ϵ-capture (ex)	^{10}C β-decay
LO	2.168(2.174)	2.294(2.334)	2.083(2.150)	2.032(2.062)
N4LO	$3.73(3.03)\times10^{-2}$	$6.07(4.98)\times10^{-2}$	$4.63(4.63)\times10^{-2}$	$1.61(1.55)\times10^{-2}$
N4LO*	$3.62(3.43)\times10^{-2}$	$6.62(5.43)\times10^{-2}$	$5.31(5.38)\times10^{-2}$	$1.80(1.00)\times10^{-2}$
MEC	$6.90(4.57)\times10^{-2}$	$10.5(10.3)\times10^{-2}$	$8.88(8.99)\times10^{-2}$	$5.31(4.28)\times10^{-2}$
EXP	2.1609(40)	2.3556(47)	2.1116(57)	1.8331(34)

TABLE I. Gamow-Teller RMEs in $A=6$, 7, and 10 nuclei obtained with chiral axial currents and GFMC (VMC) wave functions corresponding to the AV18+IL7 Hamiltonian model. Results corresponding to the one-body LO contribution (row labeled LO) and to the sum of all corrections beyond LO obtained with cutoff Λ=500 MeV and 600 MeV (rows labeled respectively as N4LO and N4LO*), are listed. The sum of all two-body corrections obtained with conventional meson-exchange axial currents is listed in the row labeled MEC. Cumulative contributions, to be compared with the experimental data [14, 32–34] reported in the last row, are obtained by adding to the LO terms the contributions from either the chiral (N4LO or N4LO*) or the conventional (MEC) currents. Statistical errors associated with the Monte Carlo integrations are not shown, but are $\sim 1\%$.

The sum of all contributions beyond LO, denoted as N4LO and N4LO* in Table I, leads approximately to a 2–3% increase in the LO prediction for the GT matrix elements of all processes under consideration. There is some cutoff dependence in these contributions, as indicated by the difference between the rows labeled N4LO and N4LO* in Table I, which may be aggravated here by the lack of consistency between the χEFT currents and the phenomenological potentials used to generate the wave functions, *i.e.*, by the mismatch in the short-range behavior of potentials and currents. The N4LO and N4LO* results in Table I correspond to the set $(c_3, c_4)=(-3.2,5.4)$ GeV^{-1} [29] in the OPE GT operator at N3LO. To illustrate the sensitivity of predictions to the set of (c_3, c_4) values, we observe that use of the more recent determination $(c_3, c_4)=(-5.61,4.26)$ GeV^{-1} [30] would lead to an N4LO GFMC-calculated value of $6.71(2.89)\times10^{-2}$ for the ^{7}Be ϵ capture to the ^{7}Li ground (first excited) state for the choice of cutoff $\Lambda = 500$ MeV, to be compared to the corresponding $6.07(4.63)\times10^{-2}$ reported in Table I. Lastly, the N4LO contributions obtained with the more accurate GFMC wave functions are about 20% larger than those corresponding to VMC wave functions for the ^{6}He and ^{7}Be-to-^{7}Li ground-state transitions, albeit it should be emphasized that this is in relation a small overall $\sim 2\%$ correction from 2b and 3b operators.

	gs	ex
LO	2.334	2.150
N2LO	-3.18×10^{-2}	-2.79×10^{-2}
N3LO(CT)	2.79×10^{-1}	2.36×10^{-1}
OPE	-2.99×10^{-2}	-2.44×10^{-2}
N4LO(2b)	-1.61×10^{-1}	-1.33×10^{-1}
N4LO(3b)	-6.59×10^{-3}	-4.86×10^{-3}

TABLE II. Individual contributions to the ^{7}Be ϵ-capture Gamow-Teller RMEs obtained at various orders in the chiral expansion of the axial current ($\Lambda = 500$ MeV) with VMC wave functions. The rows labeled LO and N2LO refer to, respectively, the first term and the terms proportional to $1/m^2$ in Eq. (1); the rows labeled N3LO(CT) and OPE, and N4LO(2b) and N4LO(3b), refer to panel (a) and panels (b) and (f), and to panels (c)-(e), (g) and panel (h) in Fig. 1, respectively.

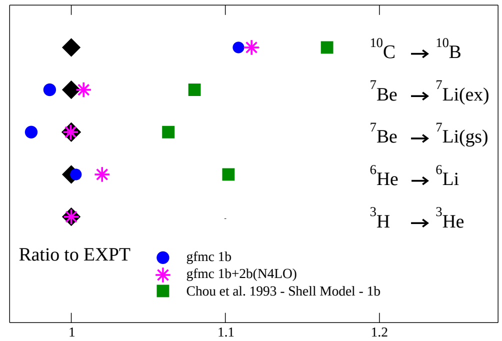

FIG. 2. (Color online) Ratios of GFMC to experimental values of the GT RMEs in the ^{3}H, ^{6}He, ^{7}Be, and ^{10}C weak transitions. Theory predictions correspond to the χEFT axial current in LO (blue circles) and up to N4LO (magenta stars). Green squares indicate 'unquenched' shell model calculations from Ref. [14] based on the LO axial current.

The contributions of the axial current order-by-order in the chiral expansion are given for the GT matrix element of the ^{7}Be ϵ capture in Table II. Those beyond LO, with the exception of the CT at N3LO, have opposite sign relative to the (dominant) LO. The loop corrections N4LO(2b) are more than a factor 5 larger (in magnitude) than the OPE. This is primarily due to the accidental cancellation between the terms proportional to c_3 and c_4 in the OPE operator at N3LO (which also occurs in the tritium GT matrix element [27]). It is also in line with the *chiral filter hypothesis* [35–37], according to which, if soft-pion processes are suppressed—as is the case for the axial current—then higher-order chiral corrections are not necessarily small. Indeed, the less than 3% overall correction due to terms beyond LO reported in Table I (row N4LO) comes about because of destructive interference between two relatively large ($\sim 10\%$) contributions from the CT and the remaining [primarily N4LO(2b)] terms considered here.

Ratios of GFMC to experimental values for the GT RMEs in the ^{3}H, ^{6}He, ^{7}Be, and ^{10}C weak transitions are displayed in Fig. 2—theory results correspond to χEFT axial currents at LO and including corrections up to N4LO. The experimental values are those listed in Table I, while that for ^{3}H is 1.6474(24) [27]. These values have been obtained by using $g_A = 1.2723(23)$ [38] and $K/\left[G_V^2\left(1+\Delta_R^V\right)\right] = 6144.5(1.4)$ sec [39], where $K = 2\,\pi^3 \ln 2/m_e^5 = 8120.2776(9) \times 10^{-10}$ GeV^{-4} sec and $\Delta_R^V = 2.361(38)\%$ is the transition-independent radiative correction [39]. In the case of the β decays, but not for the ϵ captures, the transition-dependent (δ'_R) radiative correction has also been accounted for. Lastly, in the ϵ processes the rates have been obtained by ignoring the factors B_K and B_{L1} which include the effects of electron exchange and overlap in the capture from the K and $L1$ atomic subshells. As noted by Chou *et al.* [14] following Bahcall [40, 41], such an approximation is expected to be valid in light nuclei, since these factors only account for a redistribution of the total strength among the different subshells (however, it should be noted that B_K and B_{L1} were retained in Ref. [11], and led to the extraction of experimental values for the GT RMEs about 10% larger than reported here).

We find overall good agreement with data for the ^{6}He β-decay and ϵ captures in ^{7}Be, although the former is overpredicted by $\sim 2\%$, a contribution that comes almost entirely from 2b and 3b chiral currents. The experimental GT RME for the ^{10}C β-decay is overpredicted by $\sim 10\%$, with two-body currents giving a contribution that is comparable to the statistical GFMC error. We note that correlations in the wave functions significantly reduce the matrix elements, a fact that can be appreciated by comparing the LO GFMC (blue circles in Fig. 2) and the LO shell model calculations (green squares in the same figure) from Ref. [14]. Moreover, preliminary variational Monte Carlo studies, based on the Norfolk two- and three-nucleon chiral potentials [6, 42, 43] and the LO GT operator, bring the ^{10}C prediction only $\sim 4\%$ above the experimental datum [44], indicating that the $\sim 10\%$ discrepancy we find here may be attributable to deficiencies in the AV18+IL7 wave functions of $A = 10$ nuclei.

In the present study we have shown that weak transitions in $A = 6$–10 nuclei can be satisfactorily explained in the basic model, without having to "quench" g_A. Clearly, in order to resolve the mismatch in the short-range behavior between potentials and currents alluded to earlier, GFMC calculations based on the Norfolk chiral potentials of Refs. [6, 43] and consistent chiral currents are in order. Work along these lines is in progress.

Correspondence with I.S. Towner in reference to radiative corrections in the $A = 6$–10 weak transitions is gratefully acknowledged. The work of S.P., J.C., S.G., S.C.P., and R.B.W. has been supported by the NUclear Computational Low-Energy Initiative (NUCLEI) SciDAC project. This research is also supported by the U.S. Department of Energy, Office of Science, Office of Nuclear Physics, under contracts DE-AC05-06OR23177 (R.S.), DE-AC02-06CH11357 (S.C.P. and R.B.W.), and DE-AC52-06NA25396 and Los ALamos LDRD program (J.C. and S.G.). Computational resources have been provided by Los Alamos Open Supercomputing, and Argonne's Laboratory Computing Resource Center. We also used resources provided by NERSC, which is supported by the US DOE under Contract DE-AC02-05CH11231.

[1] J. Carlson and R. Schiavilla, Rev. Mod. Phys. **70**, 743 (1998) and references therein.
[2] S. Bacca and S. Pastore, J. Phys. G: Nucl. Part. Phys. **41**, 123002 (2014) and references therein.
[3] J. Carlson, S. Gandolfi, F. Pederiva, S.C. Pieper, R. Schiavilla, K.E. Schmidt, and R.B. Wiringa, Rev. Mod. Phys. **87**, 1067 (2015) and references therein.
[4] L.E. Marcucci, K.M. Nollett, R. Schiavilla, and R.B. Wiringa, Nucl. Phys. **A777**, 111 (2006) and references therein.
[5] E.G. Adelberger *et al.*, Rev. Mod. Phys. **83**, 195 (2011) and references therein.
[6] M. Piarulli, A. Baroni, L. Girlanda, A. Kievsky, A. Lovato, E. Lusk, L.E. Marcucci, S.C. Pieper, R. Schiavilla, M. Viviani, and R.B. Wiringa, arXiv:1707.02883.
[7] S. Pastore, S.C. Pieper, R. Schiavilla, and R.B. Wiringa, Phys. Rev. C **87**, 035503 (2013).
[8] R. Schiavilla, R.B. Wiringa, S.C. Pieper, and J. Carlson, Phys. Rev. Lett. **98**, 132501 (2007).
[9] R.B. Wiringa, R. Schiavilla, S.C. Pieper, and J. Carlson, Phys. Rev. C **89**, 024304 (2014).
[10] L.E. Marcucci, F. Gross, M.T. Pena, M. Piarulli, R. Schiavilla, I. Sick, A. Stadler, J.W. Van Orden, and M. Viviani, J. Phys. G: Nucl. Part. Phys. **43**, 023002 (2016).
[11] R. Schiavilla and R.B. Wiringa, Phys. Rev. C **65**, 054302 (2002).
[12] M. Pervin, S.C. Pieper, and R.B. Wiringa, Phys. Rev. C **76**, 064319 (2007).
[13] S. Vaintraub, N. Barnea, and D. Gazit, Phys. Rev. C **79**, 065501 (2009).
[14] W.-T. Chou, E.K. Warburton, B.A. Brown, Phys. Rev. C **47**, 163 (1993).
[15] J. Engel and J. Menendez, Reports on Progress in Physics **80**, 046301 (2017) and references therein.
[16] W.C. Parke, A. Ghovanlou, C.T. Noguchi, M. Rajan, and D.R. Lehman, Phys. Lett. B **74**, 158 (1978).
[17] H. Walliser, Q.K.K. Liu, H. Kanada, Y.C. Tang, Phys. Rev. C **28**, 57 (1983).
[18] F.J. Bartis, Phys. Rev. **132**, 1763 (1963).
[19] G. Shen, L.E. Marcucci, J. Carlson, S. Gandolfi, and R. Schiavilla, Phys. Rev. C **86**, 035503 (2012).
[20] S. Weinberg, Phys. Lett. B **251**, 288 (1990); Nucl. Phys. B **363**, 3 (1991); Phys. Lett. B **295**, 114 (1992).
[21] T.-S. Park, D.-P. Min, and M. Rho, Phys. Rep. **233**, 341 (1993); T.-S. Park, L.E. Marcucci, R. Schiavilla, M. Viviani, A. Kievsky, S. Rosati, K. Kubodera, D.-P. Min, and M. Rho, Phys. Rev. C **67**, 055206 (2003).
[22] T.-S. Park, D.-P. Min, and M. Rho, Nucl. Phys. A **596**, 515 (1996).
[23] A. Baroni, L. Girlanda, S. Pastore, R. Schiavilla, and M. Viviani, Phys. Rev. C **93**, 015501 (2016); **93**, 049902(E) (2016); **95**, 059901(E) (2017).
[24] H. Krebs, E. Epelbaum, and U.-G. Meissner, Ann. Phys. **378**, 317 (2017).
[25] R.B. Wiringa, V.G.J. Stoks, and R. Schiavilla, Phys. Rev. C **51**, 38 (1995).
[26] S.C. Pieper, AIP Conf. Proc. **1011**, 143 (2008).
[27] A. Baroni, L. Girlanda, A. Kievsky, L.E. Marcucci, R. Schiavilla, and M. Viviani, Phys. Rev. C **94**, 024003 (2016); **95**, 059902 (E) (2017).
[28] N. Fettes, U.-G. Meissner, M. Mojzis, and S. Steininger, Ann. Phys. (N.Y.) **283**, 273 (2000); **288**, 249(E) (2001).
[29] R. Machleidt and D.R. Entem, Phys. Rep. **503**, 1 (2011).
[30] M. Hoferichter, J. Ruiz de Elvira, B. Kubis, and U.-G. Meissner, Phys. Rev. Lett. **115**, 192301 (2015).
[31] B.S. Pudliner, V.R. Pandharipande, J. Carlson, and R.B. Wiringa, Phys. Rev. Lett. **74**, 4396 (1995).
[32] A. Knecht *et al.*, Phys. Rev. Lett. **108**, 122502 (2012).
[33] W. Bambynek, H. Behrens, M.H. Chen, B. Crasemann, M.L. Fitzpatrick, K.W.D. Ledingham, H. Genz, M. Mutterer, and R.L. Intemann, Rev. Mod. Phys. **49**, 78 (1977).
[34] I.S. Towner, private communication.
[35] K. Kubodera, J. Delorme, and M. Rho, Phys. Rev. Lett. **40**, 755 (1978).
[36] M. Rho, Phys. Rev. Lett. **66**, 1275 (1991).
[37] M. Rho, *Chiral Nuclear Dynamics: From Quarks to Nuclei to Compact Stars* (World Scientific Publishing, Singapore, 2008).
[38] C. Patrignani *et al.* (Particle Data Group), Chin. Phys. C **40**, 100001 (2016).
[39] J.C. Hardy and I.S. Towner, Phys. Rev. C **91**, 025501 (2015).
[40] J.N. Bahcall, Phys. Rev. C **129**, 2683 (1963).
[41] J.N. Bahcall, Rev. Mod. Phys. **50**, 881 (1978).
[42] M. Piarulli, L. Girlanda, R. Schiavilla, R. Navarro Prez, J.E. Amaro, and E. Ruiz Arriola, Phys. Rev. C **91** (2015), 024003.
[43] M. Piarulli, L. Girlanda, R. Schiavilla, A. Kievsky, A. Lovato, L.E. Marcucci, S.C. Pieper, M. Viviani, and R.B. Wiringa, Phys. Rev. C **94**, 054007 (2016).
[44] M. Piarulli, private communication.